

Gravel Effect on Wastewater Infiltration from Septic System Trenches

D. E. Radcliffe,* L. T. West, and J. Singer

ABSTRACT

Septic systems have been developed that use a chamber rather than gravel in drain line trenches. Gravel is thought to impede infiltration due to a masking effect, a reduction in biomat hydraulic conductivity when the gravel is embedded, or due to fine particles that wash off the gravel and form a low-conductivity layer, but results from studies on the effect of gravel have varied. Our objective was to determine the effect of gravel masking and embedded gravel on water flow in septic system trenches. We used the finite-element numerical model HYDRUS-2D for our analysis. We simulated water movement from the trench bottom into the Bt1 and BC horizons of a Cecil soil. Gravel masking generally had little effect. In the BC horizon where the biomat hydraulic conductivity was one order of magnitude less than that of the soil, embedded gravel produced a chamber-to-gravel system infiltration ratio of 1.50. When sidewall flow was included in the BC horizon, the effect of embedded gravel was lessened and the infiltration ratio dropped to 1.33. In the Bt1 horizon where the biomat hydraulic conductivity was four orders of magnitude less than that of the soil, embedded gravel had more of an effect, producing an infiltration ratio of 1.93, close to the manufacturer's claim that chamber systems have twice the infiltration rate of gravel systems. When sidewall flow was included in the Bt1 horizon, the effect of gravel was diminished with an infiltration ratio of 1.70. Gravel had less of an effect than claimed by the manufacturer of the chamber system because lateral gradients pulling water into the areas beneath gravel particles compensated, in part, for the reduced cross-sectional area available for infiltration in the gravel systems.

SEPTIC SYSTEMS usually consist of a tank and a drainfield where effluent infiltrates into the soil. In standard systems, the drainfield consists of a trench partially filled with gravel surrounding a perforated drain line. Chamber systems have been developed for septic systems that, unlike standard systems, do not use gravel in the trench bottom. The supposed disadvantage of gravel systems is that gravel impedes infiltration in several ways (Siegrist, 1987). Gravel particles may mask part of the soil surface at the bottom of a trench, preventing infiltration in these areas. Gravel particles may compact or become embedded in the soil or in the biomat that forms at the trench-soil interface and reduce the hydraulic conductivity of this layer. Fine particles that wash off coarse gravel particles may form a low-conductivity layer at the trench-soil interface. In Georgia, chamber systems have been approved by the State Department of Human Resources for installation using half the drain line length of gravel systems based on the

manufacturer's claim that infiltration rates are twice that of gravel systems (Infiltrator Systems, 2004).

Conclusions have varied among the studies that have looked at the effect of gravel. Beach (2001) conducted a column study using sand. There were two surface treatments, with and without gravel. For the gravel treatment, a 1-cm layer of sand was removed from the top, a layer of washed gravel (2-cm diameter) was placed on the surface, dry sand was used to fill in the void spaces, and more gravel was added to a height of 10 cm above the soil surface. Before starting wastewater application, the saturated hydraulic conductivity (K_s) of columns was measured and the average K_s was not statistically different between gravel and gravel-free columns. Columns were dosed with wastewater for 138 d. The mean final discharge rate for the gravel-free treatment was over twice the gravel treatment.

Amerson et al. (1999) found no effect of gravel masking or compaction on wastewater infiltration rates. They did find an effect due to fine particles associated with gravel in one of two soils. They used large gravel (3-cm median diameter) and small gravel (1-cm median diameter). Fines used in this study were collected by washing gravel samples obtained commercially from six suppliers and comprised 1 to 4% of the gravel mass. Fines had sandy loam texture and were applied at a rate that simulated the total amount that would be derived from 15 cm of gravel with 5% fines by weight.

Bouma (1975) described a method to estimate steady infiltration rates through a trench bottom with a well-developed biomat. His analysis assumed flow through the biomat and underlying soil was steady and one-dimensional, and a unit hydraulic gradient occurred in the underlying soil (only gravity caused flow). Under these conditions:

$$Q_b = \frac{\Delta H}{R_b} = K_b \frac{h_0 - h_s + Z_b}{Z_b} \quad [1]$$

where Q_b is the steady flow rate through the biomat (cm d^{-1}), ΔH is the change in total head across the biomat (cm), R_b is the hydraulic resistance of the biomat (d), K_b is the biomat unsaturated or saturated (depending on the pressure head in the biomat) hydraulic conductivity (cm d^{-1}), h_0 is the depth of ponding in the trench (cm), h_s is the matric head ($h_s < 0$) in the soil beneath the biomat (cm), and Z_b is the biomat thickness (cm). Flow through the soil beneath the biomat (Q_s) was described by:

$$Q_s = K(h_s) \quad [2]$$

where $K(h_s)$ is the unsaturated hydraulic conductivity of the soil at a matric head of h_s . At steady state, $Q_s = Q_b$ and (assuming we know the unsaturated hydraulic conductivity function, K_b , and the depth of ponding) the only unknown is h_s . Flow through the biomat (Eq. [1])

D.E. Radcliffe and L.T. West, Crop and Soil Sciences Dep., Univ. of Georgia, Athens, GA 30602; J. Singer, Savannah River Ecology Lab, Aiken, SC 29803. Received 9 Sept. 2004. *Corresponding author (dradclif@uga.edu).

Published in Soil Sci. Soc. Am. J. 69:1217–1224 (2005).

Soil Physics

doi:10.2136/sssaj2004.0302

© Soil Science Society of America

677 S. Segoe Rd., Madison, WI 53711 USA

will increase as h_s becomes more negative. On a plot of $K(h_s)$ and flow through the biomat (Eq. [1]) as a function of h_s , the point where the curves intersected gave the steady flow rate (Eq. [2]) and the matric head in the underlying soil at steady state (see our later Fig. 5 and Fig. 7 as examples).

Bouma (1975) also measured steady infiltration rates in 13 septic system trenches and used tensiometers to determine the soil matric head. Assuming a unit hydraulic gradient, he calculated R_b of the bottom biomats, which ranged from 4.6 to 9000 d. Using a biomat thickness of 2 cm (which Bouma observed to be typical), the biomat hydraulic conductivities can be calculated from these data. They ranged from 0.0002 to 0.435 cm d⁻¹ with a mean value of 0.048 cm d⁻¹.

Soil water flow in septic system trenches in most cases is not one dimensional or steady. It also includes areas of unsaturated and saturated flow, especially in the region where biomats form. This type of flow is especially suitable to analysis using two-dimensional numerical models for unsaturated and saturated water flow. The USEPA has called for the use of these types of models to better understand wastewater treatment in septic systems (Electric Power Research Institute, 2000).

Beach and McCray (2003) used HYDRUS-2D to model water flow in a chamber system. They assumed a biomat formed on both the bottom and sidewalls of the trench and that the biomat thickness was 3 cm on the bottom and 2 cm on the sidewall. Four scenarios were considered: a coarse sandy soil with a high and low biomat K_b and a silt soil with a high and low biomat K_b . The K_s of the coarse sand was 2000 cm d⁻¹ and the K_s of the silt was 40 cm d⁻¹. The high biomat K_b was 6.0 cm d⁻¹ for the bottom and 7.44 cm d⁻¹ for the sidewall. The low biomat K_b was 1.5 cm d⁻¹ for the bottom and 2.16 cm d⁻¹ for the sidewall. As such, the biomat K_b ranged from one to three orders of magnitude less than the soil K_s . Their model results showed that an unsaturated zone formed beneath the trench when the biomat was present. Sidewall flow was most evident in the coarse sand with a low conductivity biomat. In the silt soil, where there was less of a difference between the biomat and soil hydraulic conductivities, a biomat had less effect.

We think that deterministic, two-dimensional, numerical models of unsaturated and saturated water flow can be useful in comparing septic systems with different geometries, as demonstrated by Beach and McCray (2003). The models may not predict accurate absolute values for infiltration, for example, unless they are calibrated (HYDRUS-2D has an inverse capability suitable

for calibration). But if they are used to compare systems with different geometries, they are likely to show accurate relative differences between systems. The spatial scale of septic systems is on the order of meters and this seems appropriate for a deterministic approach, whereas a stochastic approach might be required for larger spatial scales. Simulating preferential flow is a challenge for deterministic models based on the Richards equation (although HYDRUS-2D allows stochastic scaling of soil hydraulic properties), but biomats in septic trenches induce unsaturated flow immediately below the trench and this makes macropore flow less likely, as noted by Beach and McCray (2003).

Our objective was to use HYDRUS-2D to determine the effect of gravel masking and embedded gravel in septic system trenches. We did not attempt to model the effect of gravel fines.

MATERIALS AND METHODS

HYDRUS-2D is a two-dimensional finite element model for simulating the movement of water, heat, and solutes in variably saturated media (Simunek et al., 1998). Water retention and hydraulic conductivity functions must be specified for each soil layer in the model. Various equations are available for describing the unsaturated hydraulic conductivity function of soil layers. We used the van Genuchten (1980) equation:

$$K(h) = K_s \Theta^{0.5} [1 - (1 - \Theta^{1/m})^m]^2 \quad [3]$$

where m is a fitted parameter from the water retention curve (see Eq. [5] below) and relative water content (Θ) is defined as:

$$\Theta = \frac{\theta - \theta_r}{\theta_s - \theta_r} \quad [4]$$

where θ is the volumetric water content (cm³ cm⁻³), θ_s is the saturated volumetric water content (cm³ cm⁻³), and θ_r is the residual volumetric water content (cm³ cm⁻³). We simulated a septic system installation in a Cecil soil. The Cecil is a common soil in the southern Piedmont, occupying 15% of the soils mapped in the region (Radcliffe and West, 2000). Bruce et al. (1983) reported water retention data and hydraulic conductivities for a number of Cecil pedons. The horizon depths, textures, and saturated hydraulic conductivities for one of the pedons (Plot 4) are shown in Table 1. Using the Minerr function in Mathcad (Mathsoft, 2002), the data for each horizon from Plot 4 were fitted to the van Genuchten (1980) equation for water retention:

$$\Theta = (1 + |\alpha h|^n)^{-m} \quad [5]$$

where θ_r , α , and n were fitted parameters and it was assumed that $m = 1 - 1/n$ as suggested in van Genuchten (1980). Fitted values of θ_r , α , and n are shown in Table 1. We assumed that

Table 1. Horizon depths, textures, saturated hydraulic conductivities (K_s), and water retention parameters† of a Cecil pedon (Plot 4) from Bruce et al. (1983).

Horizon	Depth cm	Texture	K_s cm d ⁻¹	θ , cm ³ cm ⁻³		α cm ⁻¹	n
				θ_r	θ_s		
Ap	0–21	loamy sand	460.6	0.036	0.399	0.0499	1.468
BA	21–26	sandy clay	184.6	0.159	0.342	0.1360	1.289
Bt1	26–102	clay	257.5	0.235	0.436	0.0554	1.175
Bt2	102–131	clay	4.94	0.0	0.424	0.0066	1.085
BC	131–160	clay loam	0.84	0.0	0.423	0.0043	1.137
C	160–250+	sandy clay loam	11.20	0.080	0.445	0.0050	1.361

† θ_r , saturated volumetric water content; θ_s , residual volumetric water content; α and n , fitted parameters.

θ_s was equal to porosity, which we calculated from bulk density using an assumed particle density of 2.65 g cm^{-3} . The best fit to the data produced $\theta_r = 0$ in the Bt2 and BC horizons. Such low residual water contents are not realistic, but our model simulations were confined to the wet end of the curve ($h > -210 \text{ cm}$) where the fit to the data was excellent.

The typical septic system installation in the Georgia Piedmont would be to place the bottom of the trench in the BC horizon below finer-textured Bt horizons, based on the assumption that the fine-textured horizons have the lowest K_s in the profile. This assumption is often erroneous for the Cecil soil. As shown by the data from Bruce et al. (1983), the upper Bt horizons have a relatively high K_s due to good structure; the BC horizon often has the lowest saturated hydraulic conductivity. Studies on the Cecil soil in North Carolina have also shown that the depth of minimum hydraulic conductivity does not coincide with the depth of maximum clay content (Schoeneberger and Amoozegar, 1990). An alternative would be to place the trench bottom in the Bt1 horizon above the depth of minimum K_s .

We simulated water movement from the bottom of a trench into both the BC and Bt1 horizons, using the saturated hydraulic conductivity and water retention parameters for the Bt1 and BC horizons of the Cecil soil (Table 1). A list of all the configurations simulated is given in Table 2. The model space for the first simulations consisted of a block of soil at the bottom of a trench that was 30 cm wide and 60 cm deep (Fig. 1). We divided the K_s values in Table 1 by two to approximate a field-saturated hydraulic conductivity (K_b), as recommended by Bouwer (1969), so that the values we used in the model were 128.76 cm d^{-1} for the Bt1 horizon and 0.42 cm d^{-1} for the BC horizon.

The initial conditions were a profile in equilibrium with a water table at the bottom of the soil block ($h = 0$ at the water table and then h decreased by 1 cm for each cm rise in elevation above the water table). Boundary conditions on the sides of the soil block were zero flux. The boundary condition at the bottom of the soil block was a water table (pressure head of zero). The reason we chose this bottom boundary condition and a block depth of 60 cm is that septic system regulations in Georgia require that the trench bottom be installed at least 60 cm above a seasonal high water table or an impermeable or slowly permeable layer. Although the Cecil soil is normally well drained, a perched water table occurs during wet weather (Radcliffe et al., 1996).

To simulate a biomat, we used the same water retention parameters as the BC horizon, but substituted a $K_b = 0.05 \text{ cm d}^{-1}$. This value was chosen based on the research by Bouma (1975). The biomat was 2 cm in thickness. As such, the biomat hydraulic

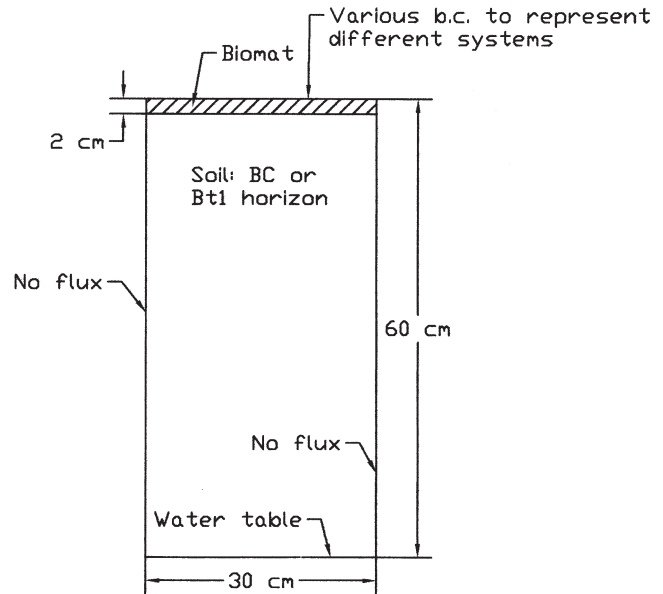


Fig. 1. Model space for chamber and gravel systems without sidewall flow.

conductivity was approximately one order of magnitude less than that of the BC horizon and four orders of magnitude less than the Bt1 horizon. The biomat layer was superimposed on the soil at the trench-soil interface. No attempt was made to integrate the biomat into the soil.

The boundary condition at the top of the block was used to differentiate between a chamber system and two configurations of a standard gravel system. For a chamber system (which would not have gravel in the trench), a constant pressure head of 5 cm, representing ponded water above the biomat, was imposed at all locations across the top of the block beginning at time zero. One configuration of a standard system was used to simulate the effect of gravel masking. This was simulated by imposing alternating no-flux boundary conditions (representing gravel particles above the biomat) and pressure heads of 5 cm (representing ponded water) across the top of the block so that 50% of the surface was designated a no-flux boundary. Each zone was 2.5 cm wide. Gravel particles were assumed to sit above the biomat and block the surface of the biomat directly below each gravel particle. The other configuration was designed to simulate the effect of gravel embedded in the biomat. In this case, gravel particles within the biomat layer were simulated by including zones 2.5 cm square with saturated hydraulic conductivities of 0.0001 cm d^{-1} (HYDRUS-2D does not allow a saturated hydraulic conductivity of zero; Rassam et al., 2003). The biomat thickness in all cases was 2 cm. We also ran simulations without a biomat to compare distributions of matric head with depth.

In a final set of simulations we examined the effect of sidewall flow. The model space for these simulations was a half-trench profile, assuming that the middle of the trench would be an axis of symmetry for two-dimensional water flow (Fig. 2). The trench bottom was placed at a depth of 150 cm below the surface on the left side of the block and the soil extended 60 cm below the trench (total depth of 210 cm). The width of the soil block from the center of the trench was 350 cm. This width was chosen to ensure that the right side of the block did not interfere with water flow. The width of the soil trench was 45 cm, half that of a full trench. Initial conditions were the same as the earlier simulations (equilibrium profile with a water table at the bottom of the model space). The boundary condition at the right and top of the soil block was

Table 2. Summary of steady infiltration rates and ratios for the chamber and gravel systems in the BC and Bt1 horizons.

System	Steady infiltration rate	Infiltration ratio to chamber
	cm d^{-1}	
BC horizon		
Chamber	0.31	
Gravel masking	0.27	1.15
Embedded gravel	0.21	1.50
Chamber with sidewall flow	0.43	
Embedded gravel with sidewall flow	0.32	1.33
Bt1 horizon		
Chamber	0.75	
Gravel masking	0.56	1.34
Embedded gravel	0.39	1.93
Chamber with sidewall flow	1.04	
Embedded gravel with sidewall flow	0.61	1.70

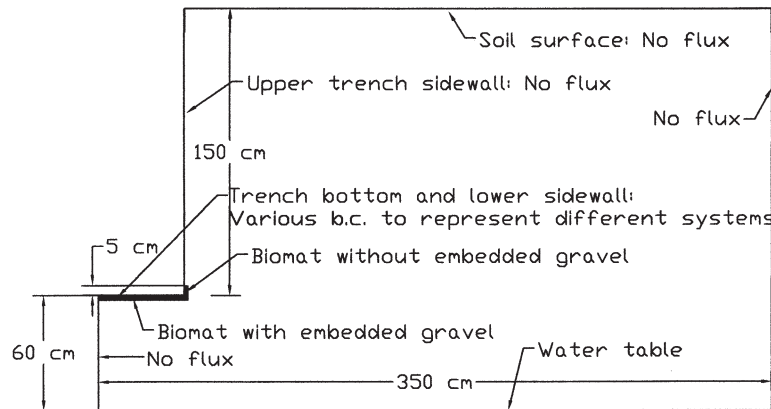


Fig. 2. Model space for chamber and gravel systems with sidewall flow.

zero flux. The boundary condition at the left below the trench was also zero flux. At the trench bottom, the same boundary conditions used in the earlier simulations to distinguish between a chamber system and two configurations of a gravel system were used (5 cm of ponded water for the chamber system, alternating 2-cm zones of zero flux and 5 cm of ponded water for gravel masking, and 5 cm of ponded water above a biomat with 2.5-cm-square zones near zero conductivity to simulate embedded gravel). On the sidewall, a 2-cm-thick biomat extended to a height 5 cm above the trench bottom. No masking or embedded gravel was simulated in the sidewall biomat.

To compare the three systems, we examined the infiltration rate into the soil over a period of 2 d. We focused on the steady infiltration rates in that they should approximate the long-term acceptance rate (LTAR) of the soils and systems we examined. The LTAR is commonly used to design septic systems and assess suitability of soils. HYDRUS-2D provides output for fluxes across each boundary in units of $\text{cm}^2 \text{d}^{-1}$. To convert to infiltration rate in cm d^{-1} , we divided the flux by the width of the trench bottom: 30 cm in the first set of simulations (Fig. 1) and 45 cm in the second set of simulations (Fig. 2).

For the 60- by 30-cm soil block (Fig. 1), we used a regular grid with a horizontal grid spacing of 0.252 cm and a vertical grid spacing of 0.25 cm. The total number of nodes was 29 880. For the model space shown in Fig. 2, we used an irregular grid with a high density in the biomat area and near the trench bottom. There were 250 nodes on the boundary and a total of 3454 nodes.

HYDRUS-2D computes an error mass balance percentage at each time step where output is requested. This is computed as the change in volume of water within the model space over a time step, less the net flux across boundaries and sinks, divided by the cumulative net flux. The model adjusts the time step to minimize the mass balance error. The error percentage in our runs was always less than 10% after the first few steps and usually less than 5%. A lower error percentage (near 1%) would have been preferred but infiltration into unsaturated soil under ponded surface conditions is a particularly difficult numerical problem (Rassam et al., 2003). We found that when a clay layer was used (in the Bt1 horizon simulations), it was critical to use the option in HYDRUS-2D specifying an air-entry value of -2 cm in the van Genuchten (1980) equations (Rassam et al., 2003).

RESULTS AND DISCUSSION

Infiltration into the BC Horizon

The infiltration rate into the BC horizon as a function of time for the simulated chamber and standard system

configurations designed to show the effect of gravel masking are shown in Fig. 3. The final steady infiltration rate is given in Table 2. For the chamber system (no gravel), the infiltration rate dropped to a steady value of 0.31 cm d^{-1} within a day. The infiltration rate in the standard system with gravel masking reached a steady rate of 0.27 cm d^{-1} within a day. As such, gravel masking had a very small effect in reducing the infiltration rate (ratio of chamber-to-gravel of 1.15, Table 2).

In Fig. 3, the infiltration rate in the BC horizon is also shown for a standard system configured to show the effect of embedded gravel. The infiltration rate in the standard system is reduced compared with that observed with gravel masking, reaching a steady rate of 0.21 cm d^{-1} . The ratio of chamber-to-gravel infiltration at the end of the period was 1.50 (Table 2). Clearly, gravel had a greater effect in reducing infiltration rates when it was embedded in the biomat. For the BC horizon, however, it was considerably less than the chamber manufacturer's claim that infiltration rates are twice as great in chamber systems as compared with gravel systems.

The reason why gravel masking had minimal effect on infiltration was that there was a large gradient at the soil surface next to gravel particles (no-flux zones) that

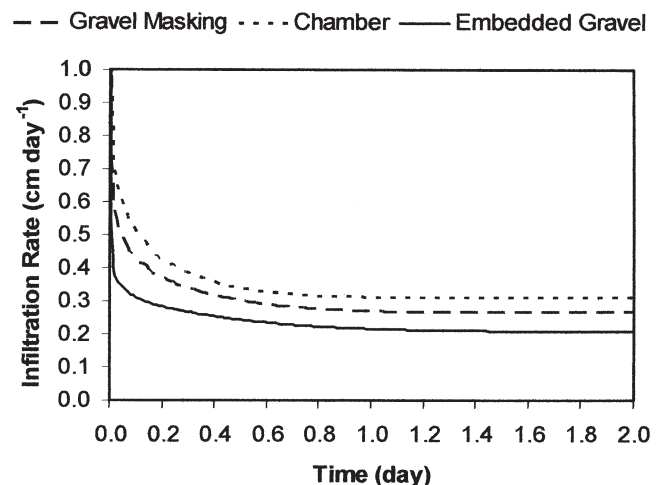


Fig. 3. Simulated infiltration rate in the BC horizon of the Cecil soil as a function of time in a chamber system and gravel systems configured to show the effect of gravel masking and embedded gravel.

pulled water laterally into the area beneath the gravel particles. This can be seen in Fig. 4 where the flux in cm d^{-1} after 1 d is shown as a function of distance along the trench–soil interface (from 0 cm at the left side of the soil block to 30 cm on the right side of the soil block). For the chamber system, the flux is a constant 0.31 cm d^{-1} . For the standard system with gravel masking half the soil surface, the flux at the surface varies between a minimum value near zero (just below the center of a gravel particle) and a maximum value of over 0.6 cm d^{-1} . The peak values occur at the edge of each open interval where the lateral gradient into the area beneath the gravel particles is greatest. Thus the higher flux between gravel particles, compared with the chamber system, compensates for the reduced cross-sectional area for infiltration in the standard system simulating the effect of gravel masking. For the standard system with embedded gravel, the flux at the surface is zero where the embedded gravel occurs and a nearly uniform flux of 0.43 cm d^{-1} between gravel particles. The lateral gradient pulling water into areas beneath the embedded gravel in this system was not as effective because these areas are more distant from the surface. As a result, the higher flux between gravel particles does not entirely compensate for the loss in infiltration surface due to embedded gravel particles.

We explored using Bouma’s (1975) approach to compare steady infiltration rates in the chamber and embedded gravel systems. In Fig. 5, we have plotted the unsaturated hydraulic conductivity function for the BC horizon in the range near saturation. We have also used Eq. [1] to plot the flux through the biomat in the chamber and embedded gravel systems. We used a biomat thickness of 2 cm (the same as our model simulations) in Eq. [1]. For the biomat K_b in the embedded gravel system, we used half the value of the chamber system ($0.05/2 = 0.025 \text{ cm d}^{-1}$) to account for embedded gravel. (We ran simulations in HYDRUS-2D to check that our soil block with a 2-cm-thick biomat layer with one-half the K_b of a chamber system had the identical infiltration rate as our embedded gravel system.) The intersection point

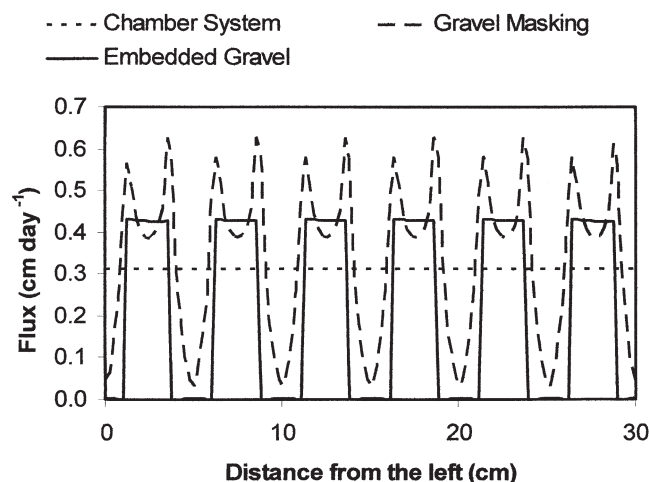


Fig. 4. Simulated flux into the BC horizon at the trench surface with the chamber system and the gravel system configured to show the effect of gravel masking and embedded gravel after 1 d.

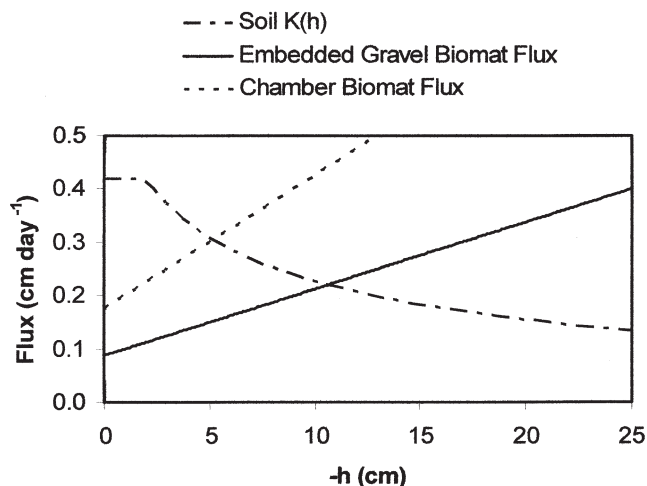


Fig. 5. Unsaturated hydraulic conductivity curve for the BC horizon and biomat flux in the chamber system and embedded gravel system (calculated from Eq. [1]) as a function of matric head in the soil beneath the biomat.

for the chamber system and the soil $K(h)$ curve occurred at a matric head of about -5 cm and the steady flux for the system was predicted to be 0.31 cm d^{-1} , identical to the HYDRUS-2D simulation (Fig. 3). For the embedded gravel system, the intersection matric head was about -10 cm and the predicted steady flux was 0.22 cm d^{-1} , very close to the HYDRUS-2D simulation of 0.21 cm d^{-1} , as well (Fig. 3). The ratio of the steady fluxes of the two systems using Bouma’s approach was 1.39, a little less than the value (1.50) obtained with HYDRUS-2D (Table 2).

Bouma’s approach worked in this case because the assumption of a unit gradient in the soil beneath the biomat was nearly true in both systems. In Fig. 6, we have plotted the matric head as a function of soil depth along a vertical transect through our soil block from the bottom of the trench to the water table 60 cm below the trench. The transects were made at the end of the simulations (2 d). For reference purposes, we ran a simulation with no biomat and the matric head distribu-

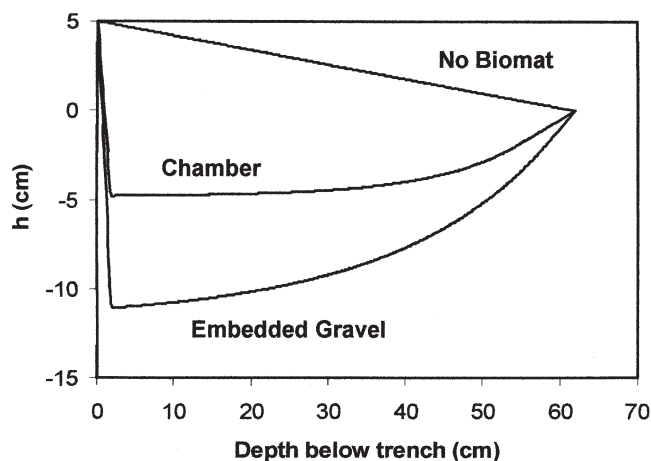


Fig. 6. Pressure (matric) head distribution in the BC soil block as a function of depth below the soil–trench interface in a simulation with no biomat, the chamber system, and the standard system configured to simulate embedded gravel at a time of 2 d.

tion along a transect in that simulation is also shown. Without a biomat, the distribution is a straight line between the boundary condition at the trench bottom (5 cm of ponded water) and the boundary condition at the bottom of the soil block (0 cm for a water table). When a biomat is present, there is a sharp drop in matric head across the biomat. Below the biomat, the matric head is nonlinear, curving from the minimum value back to a value of zero at the bottom boundary. However, immediately below the biomat there is a zone where the matric head is nearly constant, indicating that the hydraulic gradient is near unity in this region. Since the infiltration rate is steady at this time, the flux through the biomat must be equal to the soil $K(h)$, which is the assumption in Bouma's approach.

When sidewall flow was simulated (based on the model space shown in Fig. 2), steady infiltration rates for the chamber and standard systems were higher, compared with the soil block where flow occurred only through the trench bottom (Table 2). The steady infiltration rate was 0.43 cm d^{-1} in the chamber system and 0.32 in the standard system simulating embedded gravel (compared with 0.31 and 0.21 cm d^{-1} for the respective systems without sidewall flow). Sidewall flow allowed more water to infiltrate from the trench and diminished the effect of embedded gravel in that the chamber-to-gravel infiltration ratio was 1.33 (Table 2). We did not simulate the effect of sidewall flow with gravel masking, but since the effect was small in the trench bottom flow simulations (Fig. 3), we expect that it would be even less important when sidewall flow is allowed.

Infiltration into the Bt1 Horizon

When the systems were compared for infiltration into the more permeable Bt1 horizon (maintaining the same hydraulic conductivity for the biomat), more of a gravel effect was apparent. Infiltration rates reached steady state within 0.1 d, which was much quicker than in the BC horizon where steady rates were reached after about 0.5 d (Fig. 3). Overall, steady infiltration rates were much higher in the Bt1 horizon, compared with the BC horizon (Table 2). The chamber system steady infiltration rate was 1.34 times greater than the standard system with gravel masking and 1.93 times greater than the standard system with embedded gravel (Table 2). The latter ratio is close to the manufacturer's claim that infiltration rates are twice as high in chamber systems as in gravel systems.

Bouma's approach for the Bt1 horizon is shown in Fig. 7. The intersection points for the two systems and the soil $K(h)$ curve occurred at much more negative matric heads in the Bt1 horizon compared with the BC horizon: at about -53 cm in the chamber system and -66 cm in the embedded gravel system. More negative matric heads beneath the biomat are expected in this system due to the greater difference between the biomat and Bt1 horizon hydraulic conductivities. The steady flux was predicted to be 1.49 cm d^{-1} for the chamber system and 0.91 cm d^{-1} for the embedded gravel system, considerably above the steady state values predicted

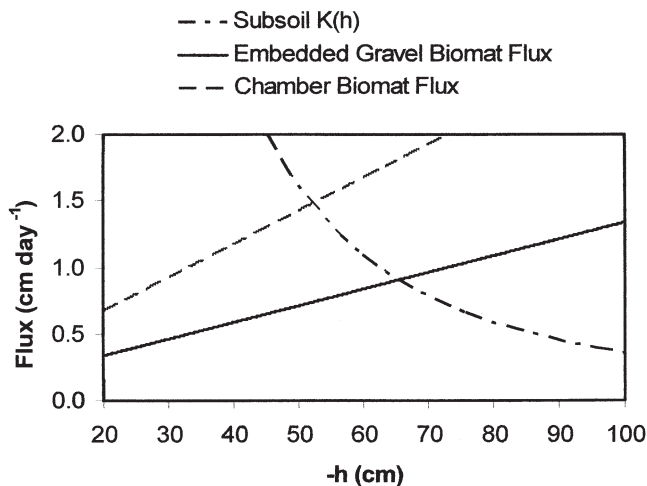


Fig. 7. Unsaturated hydraulic conductivity curve for the Bt1 horizon and biomat flux in the chamber system and embedded gravel system (calculated from Eq. [1]) as a function of matric head in the soil beneath the biomat.

by HYDRUS-2D of 0.75 and 0.39 cm d^{-1} , respectively (Table 2). The ratio was underestimated in that Bouma's analysis predicted a ratio of 1.63 compared with the ratio from HYDRUS-2D of 1.93 (chamber compared with standard system with embedded gravel, Table 2).

The reason why Bouma's analysis did not work in the Bt1 horizon is apparent in Fig. 8 where the matric head distributions as a function of depth are shown after 2 d. Unlike the BC horizon curves (Fig. 6), there is no region where matric head is constant with depth. Hence, there is no unit hydraulic gradient flow and the flux is not equal to the soil $K(h)$ beneath the biomat, violating one of the assumptions in this analysis. We suspect, however, that if the bottom boundary condition of a water table was extended to a deeper depth (more than 60 cm below the trench), the curves would flatten out and an area of unit hydraulic gradient flow would occur.

When sidewall flow was included in the Bt1 horizon (based on the model space shown in Fig. 2), infiltration rates in both systems were again higher compared with the soil block where flow occurred only through the trench bottom. The steady infiltration rate was 1.04 cm d^{-1} in the chamber system and 0.61 cm d^{-1} in the embedded gravel system (Table 2). The infiltration ratio was 1.70, again indicating that when sidewall flow was allowed, the effect of gravel was further diminished.

CONCLUSIONS

Our results show that the effect of gravel in septic system trenches varies, depending on the position of the gravel particles, on the relative difference in hydraulic conductivity of the biomat and the underlying soil, and on the degree of sidewall flow. In the BC horizon where the biomat hydraulic conductivity was one order of magnitude less than that of the soil, gravel masking had a negligible effect on the steady state infiltration rate. Embedded gravel caused an appreciable reduction in steady state infiltration in the BC horizon with the chamber system, having a steady infiltration rate 1.50 times

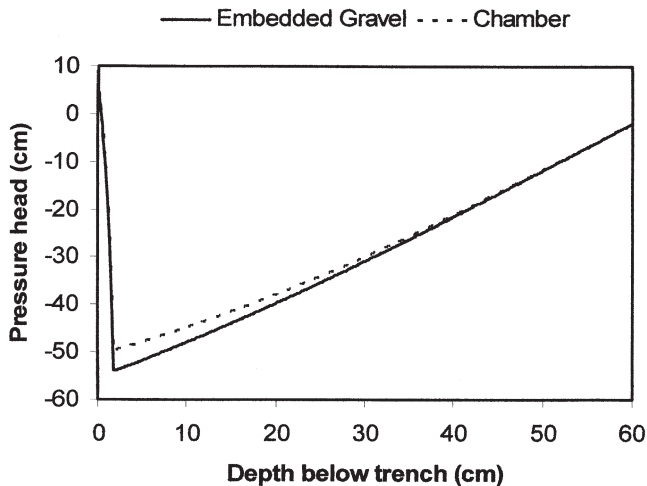


Fig. 8. Pressure (matric) head distribution in the Bt1 soil block as a function of depth below the soil-trench interface in a simulation with the chamber system and the standard system configured to simulate embedded gravel at a time of 2 d.

that for a standard system (Table 2). When sidewall flow was included in the BC horizon, the effect of embedded gravel was lessened and the infiltration ratio dropped to 1.33. In the Bt1 horizon where the biomat hydraulic conductivity was four orders of magnitude less than that of the soil, gravel had more of an effect. Gravel masking reduced steady infiltration rates somewhat so that the infiltration ratio of chamber to gravel system was 1.33. Embedded gravel further reduced infiltration rate producing an infiltration ratio of 1.93, very close to the manufacturer's claim that the chamber systems have twice the infiltration rate of gravel systems. When sidewall flow was included in the Bt1 horizon, the effect of gravel was diminished with an infiltration ratio of 1.70.

The reason why our results generally show less of an effect of gravel than claimed by the manufacturers of the chamber system is that lateral gradients pulling water into the areas beneath gravel particles compensate, in part, for the reduced cross-sectional area available for infiltration in the gravel systems. Sidewall flow also reduces the effect of embedded gravel in that the biomat on the sidewall does not include embedded gravel (our assumption). Our analysis is for two-dimensional flow. In true systems, where flow is in three dimensions, lateral gradients may be more important and there may be even less of an effect of gravel.

We used the same ponding depth of water in the trench for gravel and chamber systems. In reality, the ponding depth could be expected to be greater in gravel systems for a given dose of water, due to the volume occupied by gravel particles in the trench. This should increase infiltration in the gravel systems and further diminish differences between chamber and gravel systems. However, we did not address this effect in our simulations.

Bouma's simple analysis, based on one-dimensional steady unit hydraulic gradient flow, accurately predicted infiltration rates and ratios when the difference in biomat and soil hydraulic conductivity was small (in the BC horizon), but not when it was large (in the Bt1 horizon). This

was due to the failure to establish unit-gradient flow when there was a large difference in hydraulic conductivities and the water table was close to the bottom of the trench.

Our modeling results show that infiltration rates are most sensitive to the conditions in the biomat (masking or embedded gravel) when there is a large difference between the biomat hydraulic conductivity and soil hydraulic conductivity. This is most likely to occur in highly permeable soils such as sands. These results concur with the earlier modeling work by Beach and McCray (2003), which showed that a biomat had a greater effect in a coarse sand than in a silt.

Daniel Hillel suggested that model results cannot stand alone and that "it is only by sallying back-and-forth between experimental data and theoretical models that we can advance, albeit in a tortuous and laborious way" (Corwin et al., 1999). In that spirit, we offer the following field research questions raised by our modeling results:

- Is gravel embedded (in the biomat or soil)? If gravel is not embedded, then our results show that it has little effect on infiltration.
- What is the saturated hydraulic conductivity and thickness of biomats in soils of different textures? How do these properties change over time? To what extent do biomats form on sidewalls?
- To what extent do fines occur and what is their effect on the hydraulic properties of a biomat or a separate fines layer?
- To what extent does preferential flow occur below biomats?

REFERENCES

- Amerson, R.S., E.J. Tyler, and J.C. Converse. 1999. Infiltration as affected by compaction, fines and contact area of gravel. p. 243-247. *In Proc. of the 6th Symp. on Individual and Small Community Sewage Systems*. 16-17 Dec. 1991, Chicago IL. Am. Soc. of Agric. Eng., St. Joseph, MI.
- Beach, D.N. 2001. The use of one-dimensional columns and unsaturated flow modeling to assess the hydraulic processes in soil-based wastewater treatment systems. M.S. thesis. Colorado School of Mines, Golden.
- Beach, D.N.H., and J.E. McCray. 2003. Numerical modeling of unsaturated flow in wastewater soil absorption systems. *Ground Water Monit. Rem.* 23:64-72.
- Bouma, J. 1975. Unsaturated flow during soil treatment of septic tank effluent. *J. Environ. Eng. Div. Am. Soc. Civ. Eng.* 101:967-983.
- Bouwer, H. 1969. Infiltration of water into nonuniform soil. *J. Irrig. Drain. Div. Am. Soc. Civ. Eng.* IR4:451-462.
- Bruce, R.R., J.H. Dane, V.L. Quisenberry, N.L. Powell, and A.W. Thomas. 1983. Physical characteristics of soils in the Southern Region: Cecil. Georgia Agric. Exp. Stn., Athens, GA.
- Corwin, D.L., J. Letey, Jr., and M.L. Carillo. 1999. Modeling non-point source pollutants in the vadose zone: Back to basics. p. 323-342. *In D.L. Corwin, K. Loague, and T.R. Ellsworth (ed.) Assessment of non-point source pollution in the vadose zone*. Am. Geophys. Union, Washington, DC.
- Electric Power Research Institute. 2000. Risk-based decision making for onsite wastewater treatment. Proceedings of the Natl. Res. Needs Conf., St. Louis. 19-20 May 2000. EPRI, Palo Alto, CA.
- Infiltrator Systems. 2004. Overview [Online]. Available at www.infiltratorsystems.com/about_overview_science2.htm (verified 11 Mar. 2005). Infiltrator Systems, Old Saybrook, CT.
- Mathsoft. 2002. Mathcad. Version 11. Mathsoft, Cambridge, MA.
- Radcliffe, D.E., P.M. Tillotson, P.F. Hendrix, L.T. West, J.E. Box,

- and E.W. Tollner. 1996. Anion transport in a Piedmont Ultisol: I. Field-scale parameters. *Soil Sci. Soc. Am. J.* 60:755–761.
- Radcliffe, D.E., and L.T. West. 2000. MLRA 136: Southern Piedmont. In H.D. Scott (ed.) *Water and chemical transport in soils of the Southeastern U.S.A.* [Online]. Available at <http://soilphysics.okstate.edu/S257/book/mlra136/index.html> (verified 11 Mar. 2005). Oklahoma State Univ., Stillwater.
- Rassam, D., J. Simunek, and M. Th. van Genuchten. 2003. Modeling variably saturated flow with HYDRUS-2D. ND Consult., Brisbane, Australia.
- Schoeneberger, P., and A. Amoozegar. 1990. Directional saturated hydraulic conductivity and macropore morphology of a soil-saprolite sequence. *Geoderma* 46:31–49.
- Siegrist, R.L. 1987. Soil clogging during subsurface wastewater infiltration as affected by effluent composition and loading rate. *J. Environ. Qual.* 16:181–187.
- Simunek, J., K. Huang, and M.Th. van Genuchten. 1998. The HYDRUS code for simulating the one-dimensional movement of water, heat, and multiple solutes in variably-saturated media. Version 6.0. Res. Rep. 144. U.S. Salinity Lab., USDA-ARS, Riverside, CA.
- van Genuchten, M.Th. 1980. A closed form equation for predicting the hydraulic conductivity of unsaturated soils. *Soil Sci. Soc. Am. J.* 44:892–898.